



Adsorption of Mercury on Activated Carbon in Simulated Flue Gas with Continuous Components Change

CHANG-XING HU^{1,*}, JIN-SONG ZHOU², JIAN-XIN LI¹, YONG-CHUAN WANG¹,
JIAO ZHENG¹, MEI-JUAN XU¹, ZHONG-YANG LUO² and KE-FA CEN²

¹Ningbo Institute of Technology, Zhejiang University, Ningbo 315100, P.R. China

²State Key Laboratory of Clean Energy Utilization, Zhejiang University, Hangzhou 310027, P.R. China

*Corresponding author: E-mail: huchx@zju.edu.cn

(Received: 26 March 2013;

Accepted: 29 August 2013)

AJC-14044

This paper focused on the influence of flue gas component change on elemental mercury (Hg^0) adsorption by powder activated carbon from apricot's shell and discussed the Hg^0 adsorption characteristics and mechanism of activated carbon. Experimental results showed that activated carbon from apricot's shell had no Hg^0 adsorption ability in the non-oxidizing atmosphere, such as N_2 , $\text{N}_2 + \text{CO}_2$ etc. Though the influence on homogeneous oxidation reaction of Hg^0 was limited, NO_2 was the key factor on heterogeneous catalytic oxidation reaction of Hg^0 on the surface of activated carbon. It was easy to form NO_2 by reaction between the NO and O_2 . It could also enhance the Hg^0 adsorption ability of activated carbon through preloading NO_2 on the surface. Based on these experimental results, it finely proved that Hg^0 adsorption by activated carbon was a heterogeneous catalytic oxidation reaction.

Key Words: Apricot shell, Activated carbon, Elemental mercury, Oxidization, Chemical adsorption.

INTRODUCTION

Mercury emission from coal fired is one of the main anthropogenic mercury pollution sources. There are three types of mercury speciation existing in the flue gas, zero-valent mercury (Hg^0), bivalent mercury (Hg^{2+}) and particle mercury (Hg^p). The ratio of mercury speciation will transform with the change of flue gas components, temperature and time, etc.¹. Mercury speciation is the key influence factor on choosing the flue gas mercury control technology. Hg^0 is the main source to induce global mercury pollution, because it is difficult to be controlled for its insolubility in water and stabilization within 1-2 years in the atmosphere. Adsorbent injection mercury control technology has widely applicable and can satisfy the higher mercury emissions control standard, which can be used alone or in combination of other technologies and is one of the effective flue gas mercury control technologies.

The Hg^0 adsorption mechanism by activated carbon in different flue gas is very important for developing new low-cost carbon based adsorbents. Many papers²⁻⁹ reported the researches on mercury adsorption mechanism of carbon based adsorbents. It found that some flue gas components could always promote adsorption of mercury by activated carbon in different conditions^{10,11}. The latest research⁴ showed that in the non-oxidizing atmosphere and without oxidizing elements

on the surface, activated carbon had no Hg^0 adsorption ability and physical adsorption process did not exist between the activated carbon and Hg^0 . Further research found activated carbon had efficient Hg^0 adsorption ability in simulated flue gas and Hg^{2+} was almost the only speciation at the outlet of fixed bed when Hg^0 adsorption on activated carbon was saturated¹². It showed that the chemical oxidation adsorption existed in the process of activated carbon adsorption of Hg^0 .

This paper mainly discussed the Hg^0 adsorption characteristics of powder activated carbon from apricot's shell (AS-AC) in simulated flue gas with continuous change of components. It focused on the influence of flue gas component change on mercury adsorption by AS-AC and the mercury adsorption mechanism of activated carbon, which would be helpful to develop effective low-cost carbon-based adsorbents.

EXPERIMENTAL

Experimental setup of adsorption: The bench-scale Hg adsorption experimental setup is shown in Fig. 1 including simulated flue gas, fixed adsorption bed, flue gas Hg continuous emission monitor (CEM), conventional flue gas pollution, adsorption temperature control system and tail gas treatment, etc. The experimental setup is stable and reliable¹³.

The simulated flue gas consisted of three parts: conventional flue gas components, H_2O and Hg^0 source. The simulated

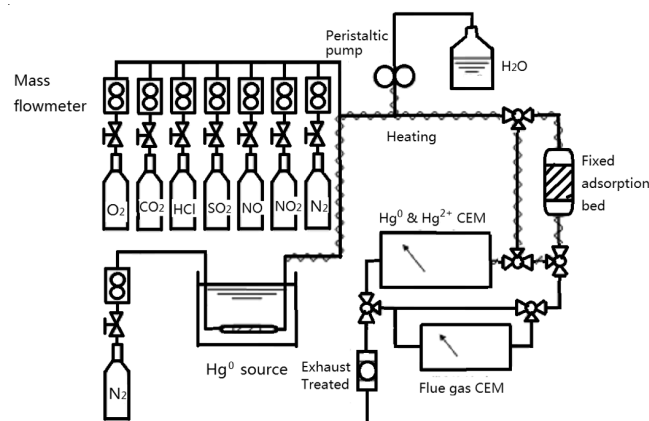


Fig. 1. Bench-scale experiment system of mercury adsorption on sorbent

conventional flue gas components, such as N_2 , CO_2 , O_2 , SO_2 , NO , NO_2 and HCl , were adjusted by mass flowmeters of the standard gas sources. H_2O was added to the simulated flue gas using a peristaltic pump which transferred water into the glass tube wrapped with heating line. Hg^0 was generated by a mercury permeation tube. The Hg^0 concentration was changed by altering the temperature of permeation tube or the flow rate of carrier gas.

The fixed adsorption bed was made by silicate glass and quartz filter, whose height was 80 mm and inner diameter was 10 mm. The pore diameter of quartz filter was less than 0.05 mm and the filter could hold the activated carbon. In this study, the AS-AC made by steam activated method was used. Steam activation is a common activation technique for AC production and is effective for creating more surface area physically by opening up more micropores. The surfaces of AS-AC had no specific active element besides some possible hydrogen and oxygen elements according to their steam activation method. The surface physical characteristics of AS-AC are given in Table-1.

TABLE-1
SURFACE PHYSICAL CHARACTERISTICS OF AS-AC

Sorbent	Specific surface area (m^2/g)	Pore volume (cm^3/g)	Micropore volume ($< 20 \text{ \AA}$) (cm^3/g)	Particle size (mm)	Porosity (%)
AS-AC	1070	0.81	0.48	0.08	57

A continuous emission monitor of DM/6A/MS/1A was used to measure mercury in experiments. The continuous emission monitor has the additional capability of determining mercury speciation in the sample gas stream. Firstly, the sample gas is washed by a potassium chloride solution to capture the divalent mercury. Secondly, the washed sample gas passes through a gas-liquid separator and a potassium hydroxide scrubber to remove interferential gases such as SO_2 . Thirdly, the remaining sample gas passes through a chiller to remove moisture and the CVAAS (cold vapour generation atomic absorption spectrometry) detector to make a measurement of gaseous Hg^0 . On the other hand, the KCl solution containing the Hg^{2+} reacts with a tin chloride solution to reduce the Hg^{2+} to the gaseous Hg^0 . The gaseous Hg^0 is transported by the carrier gas passing through a gas-liquid separator and a KOH

scrubber to remove interferential gases. After dehumidification, the carrier gas with Hg^0 passes through another CVAAS detector to make a measurement of Hg^{2+} in the flue gas stream. The CEM with automatic zero adjustment has a nominal range of $0.1-1000 \mu g/m^3$ and it is calibrated by an internal permeation device with the response time of less than 1 min and with the sensitivity of $0.1 \mu g/m^3$.

These conventional gases, CO_2 , O_2 , SO_2 , NO and NO_2 , were continuously measured by NGA 2000 MLT Series. The concentrations of HCl and H_2O were determined according to concentration and flow rate of corresponding standard gases. In the experimental system, all gas pipelines and fixed bed were heated to desired temperature. The tail gas was treated before emitting into the atmosphere.

Experimental process: The temperature of adsorption bed and gas pipelines was set at $130 \text{ }^\circ C$. The 0.0505 g AS-AC was used as the sorbent. The total flow was controlled at 1.3 L/min including 300 mL/min N_2 gas for carrying Hg^0 . The continuous change process of flue gas components was divided into 17 phases (Table-2). It shows the adsorption condition, components of simulated flue gas and the corresponding experimental time.

TABLE-2
CONTINUOUS CHANGE OF FLUE GAS COMPONENTS
DURING THE ADSORPTION PROCESS

Phase	Through FAD ^a	Components of simulated flue gas	Time (min)
1	No	$N_2+Hg^0+H_2O$	0-13
2	Yes	$N_2+Hg^0+H_2O$	14-33
3	Yes	$CO_2+N_2+Hg^0+H_2O$	34-60
4	Yes	$O_2+CO_2+N_2+Hg^0+H_2O$	61-88
5	Yes	$SO_2+O_2+CO_2+N_2+Hg^0+H_2O$	89-120
6	Yes	$NO_2+SO_2+O_2+CO_2+N_2+Hg^0+H_2O$	121-173
7	Yes	$NO+NO_2+SO_2+O_2+CO_2+N_2+Hg^0+H_2O$	174-181
8	Yes	$HCl+NO+NO_2+SO_2+O_2+CO_2+N_2+Hg^0+H_2O$	182-194
9	No	$HCl+NO+NO_2+SO_2+O_2+CO_2+N_2+Hg^0+H_2O$	195-199
10	Yes	$HCl+NO+NO_2+SO_2+O_2+CO_2+N_2+Hg^0+H_2O$	200-208
11	Yes	$HCl+NO+SO_2+O_2+CO_2+N_2+Hg^0+H_2O$	209-227
12	Yes	$HCl+NO+SO_2+CO_2+N_2+Hg^0+H_2O$	228-238
13	Yes	$HCl+SO_2+CO_2+N_2+Hg^0+H_2O$	239-292
14	Yes	$HCl+CO_2+N_2+Hg^0+H_2O$	293-312
15	Yes	$CO_2+N_2+Hg^0+H_2O$	313-323
16	Yes	$N_2+Hg^0+H_2O$	324-395
17	No	$N_2+Hg^0+H_2O$	396-400

^aFAD: fixed adsorption bed.

RESULTS AND DISCUSSION

The experimental study of Hg^0 adsorption characteristics of AS-AC in simulated flue gas with continuous change of components could be divided into three processes. The first was to add components into simulated flue gas, respectively from phase 2-8. The second was simulated flue gas passing in bypass, *i.e.*, phase 9. The third was to remove components from simulated flue gas, respectively from phase 10-16.

In the experimental process, the concentrations of five flue gas components were recorded (Fig. 2). The horizontal

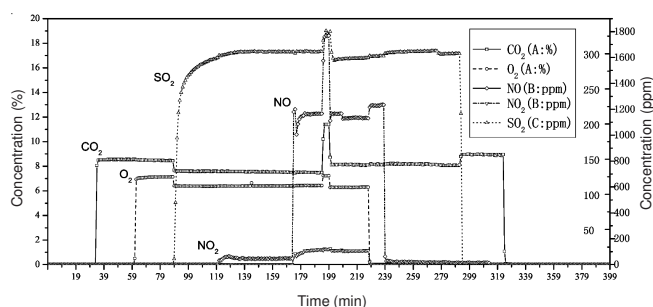


Fig. 2. Concentration change of five conventional flue gas components

ordinate denotes the experimental time (min). There are three vertical coordinates of A, B and C axis. A shows the concentrations (%) of CO_2 and O_2 ; B shows the concentrations (ppm) of NO and NO_2 ; and C shows the concentration (ppm) of SO_2 . According to the Table-2, Fig. 2 shows the outlet concentrations of fixed adsorption bed at different phases. At the 9th phase, the flue gas did not through the adsorption bed. The concentrations of HCl and H_2O were not monitored and their original concentrations were 50 ppm and 10 %, respectively.

The concentrations of Hg^0 and Hg^{2+} during the whole experimental process were shown as Fig. 3. The Hg^{2+} concentration almost did not change, which meant that no Hg^{2+} passed through the adsorption fixed bed.

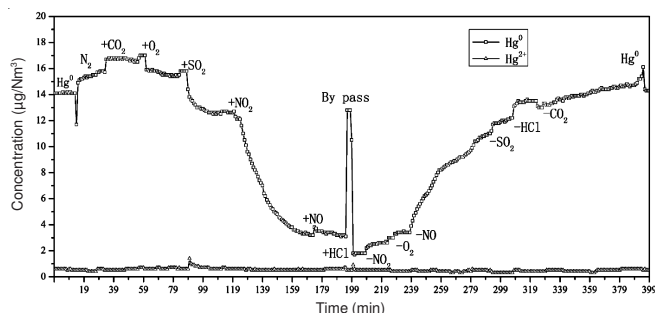
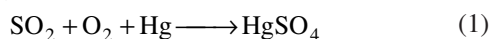


Fig. 3. Concentrations of Hg^0 and Hg^{2+} during the whole experimental process

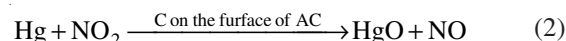
Hg^0 adsorption when flue gas components added one by one: As shown in Fig. 3, the AS-AC had no Hg^0 adsorption ability in the simulated flue gas atmosphere of N_2 , $\text{N}_2 + \text{CO}_2$, or $\text{N}_2 + \text{CO}_2 + \text{O}_2$ from the 2nd to 4th phase, which was very similar with the reported papers^{4,12}. When SO_2 was added at the 5th phase, the concentration of Hg^0 decreased a little, which meant that SO_2 could promote the Hg^0 adsorption by AS-AC. In the same time, Hg^{2+} appeared. The key point of adsorption process could be understood as reaction (1), which meant that SO_2 could oxidize the Hg^0 to Hg^{2+} with the action of O_2 on the surface of AS-AC.



At the 6th phase, the Hg^0 adsorption ability of AS-AC increased substantially when NO_2 was added. According to the concentration change of flue gas components (Fig. 2 and Table-3), the NO_2 concentration at the outlet of adsorption bed was only 0.1 ppm far less than the original NO_2 concentration of 22.2 ppm in the 9th phase. At the same time, the NO concentration at the outlet of adsorption bed was 8.7 ppm

though NO was not added in the simulated flue gas at this phase.

Many researchers¹⁴⁻¹⁸ believed that O_2 , NO_2 and NO had less effect on the gaseous homogeneous oxidizing reaction of Hg^0 because there were some restrictions of reaction kinetics among them. However, they played a key role in the heterogeneous oxidizing reaction of Hg^0 ^{19,20}. Regarding the concentration change of Hg^0 , NO_2 and NO , it could be considered that NO_2 oxidized Hg^0 on the surface of AS-AC and generated NO simultaneously. The reaction process was as the following eqn. 2.



NO was added at the 7th phase. As a result, NO_2 concentration rose from 0.1 to 14.0 ppm with the common function of O_2 through eqn. 3. The conversion efficiencies of Hg^0 to Hg^{2+} at the 6th phase and the 7th phase were almost same as 78 %. The increment of NO_2 did not further promote the Hg^0 adsorption, which was mainly because that the existing NO_2 concentration (original was 22.2 ppm) was much higher than Hg^0 concentration (ca. 14.1 $\mu\text{g}/\text{Nm}^3$). On the other hand, the increasing of NO would suppress the reaction eqn. 2.



At the 8th phase, HCl did not further promote AS-AC to adsorb Hg^0 , because it was very difficult to form active Cl by HCl in the range of experimental temperature.

Hg^0 speciation in bypass (the 9th phase): When the simulated flue gas was switched back to the bypass at the 9th phase, the Hg^0 concentration almost went back to the original Hg^0 concentration level (Fig. 3). It indicated that the influence of simulated flue gas on Hg^0 speciation was limited at the experimental temperature and Hg^0 was the dominant speciation in the simulated flue gas without the catalytic action of carbon on the surface of AS-AC. These results matched that of reference²¹. Comparing the concentrations of simulated flue gas components through the bypass and the adsorption bed, as shown in Fig. 2 and Table-3, various simulated flue gas components would always be adsorbed or changed in speciation in different degree when they passed through the AS-AC adsorption bed.

Hg^0 adsorption when flue gas components removed one by one: When the gas flow was switched from the bypass to the adsorption bed at the 10th phase, the Hg^0 concentration immediately reduced to below 2 $\mu\text{g}/\text{Nm}^3$. The conversion efficiency of Hg^0 to Hg^{2+} was ca. 85 %. In the simulated flue gas, the AS-AC showed good adsorption ability of Hg^0 . The NO_2 play the key role in promoting Hg^0 adsorption by AS-AC. During the process of flue gas components removed from simulated flue gas, respectively, NO_2 was first removed (at the 11th phase). As shown in Fig. 2, although NO_2 was removed, there was no obvious decline of NO_2 concentration, which was still hold at ca. 19.7 ppm. However, NO concentration had a slight decline. It was because the reaction (2) would happen easily when NO_2 was removed. Reaction (2) consumed more NO and produced more NO_2 simultaneously. As a result, the removal of NO_2 would not have a great influence on Hg^0 adsorption by AS-AC at this phase.

As O₂ was removed at the 12th phase, the reaction (2) stopped. Correspondingly, NO concentration had a significant rise stage and NO₂ concentration had a rapid decline to *ca.* 0.3 ppm. At the same time, as shown in Fig. 3, Hg⁰ concentration at the outlet of adsorption bed rised. The Hg⁰ oxidation ability by gaseous NO₂ disappeared gradually.

At the 13th phase, NO was removed. The Hg⁰ adsorption ability of AS-AC further dropped and Hg⁰ concentration continuously rised. However, the curve of Hg⁰ concentration was in a parabolic form because the elements of NO, NO₂ and O₂, which were already adsorbed on the surface of AS-AC through previous phases, still worked on Hg⁰ adsorption by AS-AC. The situation was quite different with Hg⁰ adsorption by AS-AC in the process when flue gas components were added, respectively. In 14th and 15th phases, SO₂ and HCl were removed sequentially, which made Hg⁰ concentration curve appear certain wave; the Hg⁰ concentration increase slightly, which meant that they both had worked on promoting of Hg⁰ adsorption.

Though all simulated components were removed after the 16th phase, the AS-AC still had the Hg⁰ adsorption ability in N₂ gas. The Hg⁰ concentration curve continuously increased in a parabolic form. It was because that the Hg⁰ adsorption was fulfilled by the components of NO, NO₂ and O₂, *etc.*, while all the components had already been adsorbed on the surface of AS-AC after nearly 3 h flue gas adsorption. It was the reason that it took *ca.* 187 min for the third process of Hg⁰ adsorption by AS-AC to reach the original concentration and the duration was *ca.* 53 min longer than that of the first phase. As shown in Fig. 3, Hg⁰ concentration curve was symmetrically distributed around the second phase.

Conclusion

According to the experimental results and discussion, it showed that the AS-AC had no Hg⁰ adsorption ability in the non-oxidizing atmosphere, such as N₂ and N₂ + CO₂, *etc.* However, the AS-AC showed strong Hg⁰ adsorption ability in the oxidizing atmosphere with NO₂ and NO, *etc.* Though the influence on homogeneous oxidation reaction of Hg⁰ was limited, NO₂ was the key factor on heterogeneous catalytic oxidation reaction of Hg⁰ on the surface of AC. It was easy to form NO₂ by reaction between the NO and O₂, which was an effective way for Hg⁰ oxidization. It also could enhance the

Hg⁰ adsorption ability of AC through preloading NO₂ on the surface. Hg⁰ adsorption by AS-AC, produced by physical method, was a complicated chemical adsorption process with the function of oxidising components of simulated flue gas and surface of AC. Based on these experimental results, it finely proved that the Hg⁰ adsorption by AC was a heterogeneous catalytic oxidation reaction.

REFERENCES

1. EPRI, An Assessment of Mercury Emissions from US Coal-Fired Power Plants, EPRI (1000608), Palo Alto, CA (2000).
2. J.S. Zhou, Z.Y. Luo, C.X. Hu and K.F. Cen, *Energy Fuels*, **21**, 491 (2007).
3. C.X. Hu, J.S. Zhou, Z.Y. Luo, S. He, G.K. Wang and K.F. Cen, *J. Environ. Sci.*, **18**, 1161 (2006).
4. C.X. Hu, J.S. Zhou, S. He, Z.Y. Luo and K.F. Cen, *Fuel Process. Technol.*, **90**, 812 (2009).
5. L.S. Xu, H.C. Zen and J. Guo, *Thermal Power Gen.*, **35**, 1 (2006).
6. E.J. Granite, M.C. Freeman, W.J. O'Dowd, R.A. Hargis and H.W. Pennline, *J. Environ. Manage.*, **84**, 628 (2007).
7. W.J. O'Dowd, H.W. Pennline, M.C. Freeman, E.J. Granite, R.A. Hargis, C.J. Lacher and A. Karash, *Fuel Process. Technol.*, **87**, 1071 (2006).
8. A.A. Presto, E.J. Granite, A. Karash, R.A. Hargis, W.J. O'Dowd and H.W. Pennline, *Energy Fuels*, **20**, 1941 (2006).
9. A.A. Presto and E.J. Granite, *Environ. Sci. Technol.*, **40**, 5601 (2006).
10. S.J. Miller, G.E. Dunham, E.S. Olson and T.D. Brown, *Fuel Process. Technol.*, **65-66**, 343 (2000).
11. T.R. Carey, O.W. Hargrove, C.F. Richardson, R. Chang and F.B. Meserole, *J. Air Waste Manage. Assoc.*, **48**, 1166 (1998).
12. C.X. Hu, J.S. Zhou, Z.Y. Luo and K.F. Cen, *Energy Fuels*, **25**, 154 (2011).
13. C.X. Hu, PhD Thesis, Mercury Emission from Coal-Fired Power Plant in China and Stability Adsorption Mechanism of Mercury on Activated Carbon, Zhejiang University, Hangzhou, China (2007).
14. B. Hall, P. Schager and E. Lindqvist, *Water Air Soil Pollut.*, **56**, 3 (1991).
15. B. Hall, E. Lindqvist and E. Ljungstrom, *Environ. Sci. Technol.*, **24**, 108 (1990).
16. B. Hall, *Water Air Soil Pollut.*, **80**, 301 (1995).
17. K.C. Galbreath and C.J. Zygarlicke, *Fuel Process. Technol.*, **65-66**, 289 (2000).
18. H.L. Hitchcock, M.S. Thesis, Mercury Sorption on Metal Oxides, University of North Dakota (1996).
19. D.V. Radisav, R.V. Joseph and U.B. Eric, Mercury Speciation in Coal-Fired Power Plant Flue Gas-Experimental Studies and Model Development Final Technical Report (August 1, 2005-July 31, 2008). Cooperative Agreement Number: DE-FG26-05NT42534 (2009).
20. G.A. Norton, H.Q. Yang, R.C. Brown, D.L. Laudal, G.E. Dunham and J. Erjavec, *Fuel*, **82**, 107 (2003).
21. C.X. Hu, J.S. Zhou, J.X. Li, Y.C. Wang, J. Zheng, M.J. Xu and Z.Y. Luo, *CIESC Journal*, **63**, 1536 (2012).